

Analysis of Crystallographic Texture and Mechanical Anisotropy of an Extruded Mg-RE Alloy

Zhai Yixuan, Hou Xiuli, Yuan Zhizhong, Zhang Peng, Guan Qingfeng

Jiangsu University, Zhenjiang 212013, China

Abstract: The impact of hot extrusion on the microstructure and texture, as well as mechanical properties of the Mg-1Gd-1Nd (wt%) alloy was investigated. The results demonstrate that the as-cast alloy displays a typical eutectic microstructure consisting of α -Mg solid solution and semi-continuous eutectic compounds. After solution treatment, the eutectic compounds are mostly dissolved in the α -Mg matrix. The microstructure and texture of the extruded alloy were analyzed by electron backscatter diffraction (EBSD) technique. It is indicated that the extruded alloy exhibits fully recrystallized microstructure and weak basal texture. In detail, the basal planes of the grains majority are spread both towards extrusion direction and transverse direction of the extruded alloy sheet. Especially in the extrusion direction, the orientation distribution is significantly dispersive. The broad spread in orientations results in effective activation of the basal slip and allows the alloy to accommodate higher strains prior to failure. On the other hand, the texture is responsible for the planar anisotropies of the extruded alloy sheet.

Key words: magnesium alloy; rare earth; EBSD; Texture; mechanical property

Magnesium alloys, as a lightweight metallic material, possess high specific strength, strong damping property, and good thermal and electrical conductivity^[1-5]. These properties have constituted magnesium alloys quite attractive for the automotive industry, as well as the computer, communication and consumer electronic (3C) appliances^[4,5]. However, compared with the widely used lightweight aluminum alloys and polymeric materials, the application of magnesium alloys is not so competitive. One important drawback for the utilization of magnesium alloys is their poor formability at ambient temperatures^[1]. It is related to the limited active slip systems of hexagonal close-packed (hcp) crystal structure and the resulting strong crystallographic textures.

During the last decade, various studies have been conducted to improve the formability of magnesium alloys through altering their textures^[6-12]. The addition of rare earth (RE) elements has been proved to be an effective way to modify the textures of wrought magnesium alloys^[8-12]. In contrast to the high alloying concentration Mg-RE alloys

that exhibit a strong precipitation hardening response, Stanford et al.^[9,10] observed that micro-alloying magnesium with RE elements can also provide obvious texture modification of the wrought alloys. Many researchers turned to the development of magnesium alloys with a dilute RE concentration from the aspect of economy. In these investigations^[10,13,14], low amounts of RE additions, usually below 2 wt%, can greatly enhance the ductility of magnesium in wrought state. Sometimes the enhanced ductility resulted in a slight compromise in strength^[14], whereas it was important for the formability improvement.

In detail, RE additions can significantly weaken the strengths of conventional textures of wrought alloys (e.g. basal texture in rolled sheets, or $\langle 10\bar{1}0 \rangle$ - $\langle 11\bar{2}0 \rangle$ fiber textures in extrusions) and alter the textures by developing new texture components, i.e. the “RE texture” components^[9-11]. Both of these changes improve the ductility of wrought magnesium alloys, leading to the enhanced formability. To date, numerous investigations have been done to explore how RE elements to control the

Received date: May 06, 2017

Foundation item: Jiangsu Province Science Foundation for Youths (BK20130519); Foundation of Jiangsu University (12JDG094)

Corresponding author: Hou Xiuli, Ph. D., School of Material Science and Engineering, Jiangsu University, Zhenjiang 212013, P. R. China, Tel: 0086-511-88797887,

E-mail: [houxiuli@ujs.edu.cn](mailto:houxuli@ujs.edu.cn)

Copyright © 2018, Northwest Institute for Nonferrous Metal Research. Published by Elsevier BV. All rights reserved.

texture evolution during thermomechanical processing. Several mechanisms including the particle stimulated nucleation (PSN)^[15,16], shear band nucleation (SBN)^[17,18], deformation twin induced nucleation (DTIN)^[19] and solute drag/pinning effect^[8] have been proposed by the researchers. However, the underlying mechanisms have not been clearly verified due to the lack of sufficient fundamental data. In this study, the Mg-1Gd-1Nd (wt%) alloy was processed by hot extrusion technique, and the rectangular extrudate was adopted instead of traditionally utilized extruded rods. The purpose of this study is to identify the crystallographic texture of the rectangular extruded alloy, elucidating the effects of RE elements on the microstructural features, as well as the mechanical behavior analysis related to the texture.

1 Experiment

The Mg-1Gd-1Nd (wt%) alloy ingot was prepared from high purity Mg (99.9 wt%), Mg-20Gd and Mg-30Nd (wt%) master alloys in an electric resistance furnace under anti-oxidizing flux protection. Subsequently to direct-chill semi-continuous casting, the ingot was machined into billets of 100 mm in diameter and solution treated for 16 h at 500 °C under a flowing argon atmosphere. Then extrusion was carried out with a ram rate of 1 mm/s at the temperature of 450 °C. The billets were extruded into sheets of 80 mm × 12 mm in dimensions on the cross section, corresponding to an area reduction ratio of 8.

Following extrusion, specimens for microstructure and texture analyses were taken from the mid-layer of extrusions in the steady state region. The microstructures were characterized by Olympus GX71 optical microscopy, scanning electron microscopy (SEM) equipped with an X-ray energy-dispersive spectrometer (EDS), and transmission electron microscopy (TEM). Texture analysis was performed on an EDAX-TSL electron backscatter diffraction (EBSD) system. Prior to EBSD analysis, the specimens were given an electrochemical polishing after standard metallographic preparation. Tensile specimens of 15 mm in the gauge length and of 5 mm in gauge width were cut along the extrusion direction (ED) and transverse direction (TD) of the sheets. Uniaxial tensile tests were carried out using WSM-50KB universal testing machine under a strain rate of $1.11 \times 10^{-3} \text{ s}^{-1}$.

2 Results and Discussion

2.1 Microstructure and texture

Optical micrographs of the as-cast and solution-treated alloys are presented in Fig.1a and Fig.1b, respectively. It can be seen that, the as-cast alloy reveals a typical eutectic microstructure consisting of α -Mg solid solution and coarse eutectic compounds, which exhibit semi-continuous network morphology crystallizing at grain boundaries. After

solution treatment, the coarse secondary phases are mostly dissolved in the α -Mg matrix and the grains become larger at the same time. Fig.2 shows the X-ray diffraction (XRD) pattern of as-cast alloy, which indicates that the eutectic compounds involve $\text{Mg}_{41}\text{Nd}_5$ and Mg_5Gd phases. According to the literatures^[2,20], the two binary phases are both stable intermediate phases in Mg-RE alloy systems. As for the Mg_5Gd phase, Nd can substitute for Gd, and thus it is commonly expressed as $\text{Mg}_5(\text{Gd},\text{Nd})$ phase^[20].

Fig.3 presents the microstructure (EBSD inverse pole figure map) and the texture (pole figures recalculated from EBSD data) of the extruded alloy. The EBSD orientation map (Fig.3a) suggests that a nearly fully recrystallized microstructure with fine equal-axial grains is formed in

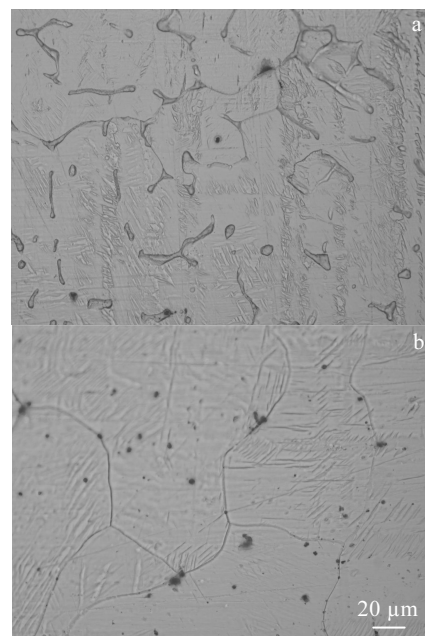


Fig.1 Optical micrographs of the as-cast (a) and solution-treated (b) alloys

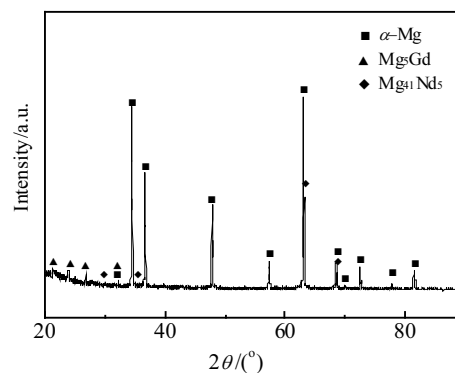


Fig.2 XRD pattern of the as-cast alloy

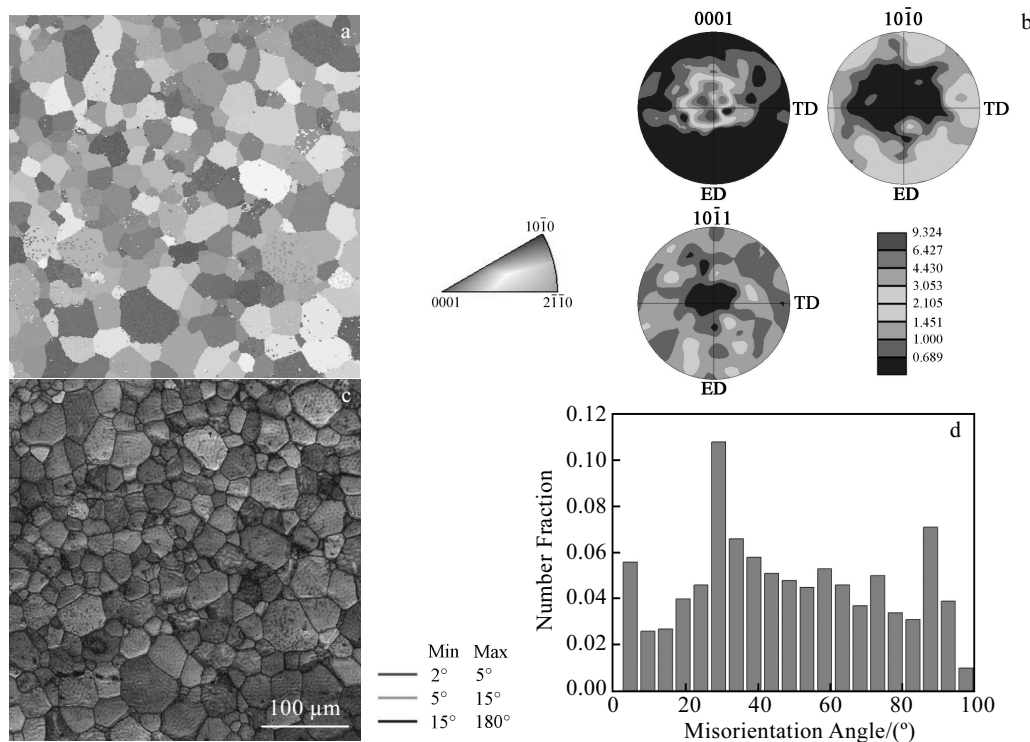


Fig.3 EBSD analysis of the extruded alloy: (a) orientation map; (b) (0001), (10 $\bar{1}$ 0) and (10 $\bar{1}$ 1) pole figures; (c) Kikuchi contrast map; (d) misorientation angle distribution

the extruded alloy. The average grain size is 34.2 μ m. Additionally, the recrystallized grains have relatively random crystallographic orientations, where the c -axes of most grains are deflected from the sheet plane normal. With respect to the pole figures (Fig.3b) of the extruded alloy, a weak and complex basal texture is observed. The (0001) basal poles are split in both the extrusion direction (ED) and transverse direction (TD) of the extruded sheet, giving four distinct intensity peaks. While for the (10 $\bar{1}$ 0) prismatic poles and (10 $\bar{1}$ 1) pyramidal poles, the intensity peaks are very weak and diffuse. The present texture results are different from those observed in conventional magnesium extrusions, where a single fiber texture <10 $\bar{1}$ 0>//ED was repeatedly reported, and sometimes the double fiber texture <10 $\bar{1}$ 0>-<1120>//ED also emerged^[21-23].

In Fig.3c, the Kikuchi contrast map shows the distribution of grain boundaries, including the high-angle grain boundaries (HAGBs) with grain misorientations $\geq 15^\circ$, low-angle grain boundaries (LAGBs) with grain misorientations in the region of $5^\circ \sim 15^\circ$, and subgrain boundaries in the region of $2^\circ \sim 5^\circ$ are depicted by blue, green and red lines. Concerning the corresponding misorientation angle distribution as shown in Fig. 3d, it is seen that the ratio of HAGBs is as high as 0.916, which means a large volume fraction of grains undergoing

dynamic recrystallization during hot extrusion processing. The low peak intensity at the low angles of 5° indicates the extent of subgrain structures within the large grains as shown in Fig.3c. Furthermore, an apparent intensity peak at the high angles of 30° is observed. The appearance of near- 30° peak is not universal in Mg alloys, but it is often observed during the growth of recrystallized grains in Mg alloys^[24], as well as in other hcp metals, such as Zr^[25] and Ti^[26] alloys. That is, the near- 30° peak emerges through a recrystallization procedure. Moreover, the intensity of near- 30° peak is correlated with the recrystallized volume fraction^[27]. For Mg alloys, the near- 30° peak is attributed to a near-coincidence site lattice (CSL) boundary $\Sigma 15a$ with a misorientation angle of about 30° , and it is responsible for the texture weakening, occurring upon the stage of grain growth in these alloys^[24].

To better detect the orientation distribution of grains in the alloy sheet, inverse pole figures with the axes in the ED, TD and normal direction (ND) are presented in Fig.4. It should be pointed out that for rectangular extruded alloys, the inverse pole figures in three vertical directions are necessary to obtain the detailed information about the texture components. It is in contrast with the round extruded alloys, where only the inverse pole figure in the ED is of importance^[9-11,19]. As shown in Fig.4, the extruded

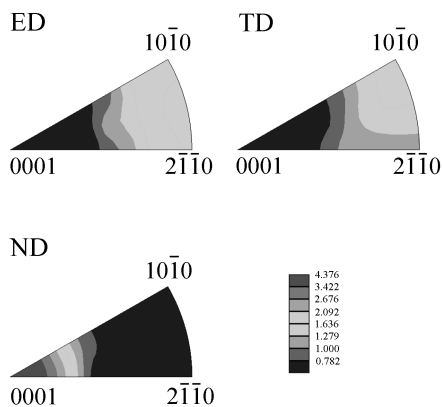


Fig.4 Texture of the extruded alloy sheet in terms of inverse pole figures in the extrusion direction (ED), transverse direction (TD) and normal direction (ND)

alloy shows a basal-type texture, where the maximum intensity is centered around $\langle 0001 \rangle$ pole in the ND, corresponding to the basal planes being mainly oriented parallel to the sheet plane. But on the other hand, the intensities spread about 30° from the $\langle 0001 \rangle$ pole towards $\langle 10\bar{1}0 \rangle$ and $\langle 11\bar{2}0 \rangle$ poles, which significantly improves the alignment of grains for basal slip and results in the enhancement of room temperature ductility. For the inverse pole figure in ED, unlike round extrusion of classical wrought magnesium alloys, there is no strong intensities found in the $\langle 10\bar{1}0 \rangle$ pole or on the arc between the $\langle 10\bar{1}0 \rangle$ and $\langle 11\bar{2}0 \rangle$ poles^[9-11,21,22]. In contrast, the orientations with moderate intensities show a spread along the arc but with an additional tilt further from the $\langle 11\bar{2}0 \rangle$ pole, i.e. towards the $\langle 11\bar{2}1 \rangle$ pole. The orientations along the arc of inverse pole figure in ED is an indication of recrystallized microstructure in which the deformed grains disappear and grain growth takes place^[28]. It is consistent with the microstructural observation in present work. Meanwhile, the tilt of orientations from $\langle 11\bar{2}0 \rangle$ pole is a unique characteristic of RE-containing magnesium extrusions,

which leads to the appearance of well known “RE texture” component $\langle 11\bar{2}1 \rangle // \text{ED}$ ^[9-11]. The inverse pole figure in TD shows a weak single $\langle 10\bar{1}0 \rangle$ component. Overall, the entire alloy sheet exhibits a weaker texture compared to conventional magnesium extrusions, such as the AZ31 alloy^[29].

2.2 Effects of RE addition on texture modification

The magnesium alloying with rare earth (RE) elements has been proved to significantly weaken the texture of wrought alloys, leading to modified alignment of grains for basal slip^[6-11]. However, the detailed mechanisms originated from RE additions regarding the texture weakening of wrought magnesium alloys are still controversial. In the last decade, the issues were mainly focused on the recrystallization behavior, because wrought magnesium alloys usually reveal a recrystallized microstructure due to the low stacking fault energy of magnesium^[10-12]. However, the latest studies have put an emphasis on the deformation behavior, and it was pointed out that the deformed microstructures forms the basis of recrystallization^[8,30]. In details, the solute drag/pinning effect produced by RE solute interactions with dislocations and grain boundaries inspires the texture modification^[30].

Fig. 5 presents the SEM image of the extruded alloy and corresponding EDX maps of the alloying elements. The distribution of Gd and Nd elements in α -Mg matrix could be clearly observed. The RE elements display significantly higher atomic radii compared to Mg, normally higher than 10% in diameter. Therefore a strong solute drag effect is produced in Mg matrix^[8]. It was reported that during thermo-mechanical processing, the solute drag effect induced by RE solute interactions with dislocations and grain boundaries controlled the texture development^[31]. In support of the solute drag effect, dynamic strain aging phenomenon occurring in RE-containing magnesium alloys is an effective evidence^[32]. As observed in the SEM image (Fig. 5), significantly fine precipitates exist at the grain boundary and grain interior, constituting good evidence of dynamic strain aging.

2.3 Tensile properties

Fig. 6 shows the tensile stress-strain (S - S) curves of the extruded alloy sheet tested along ED and TD. It is seen that the elongation along ED is obviously higher than that

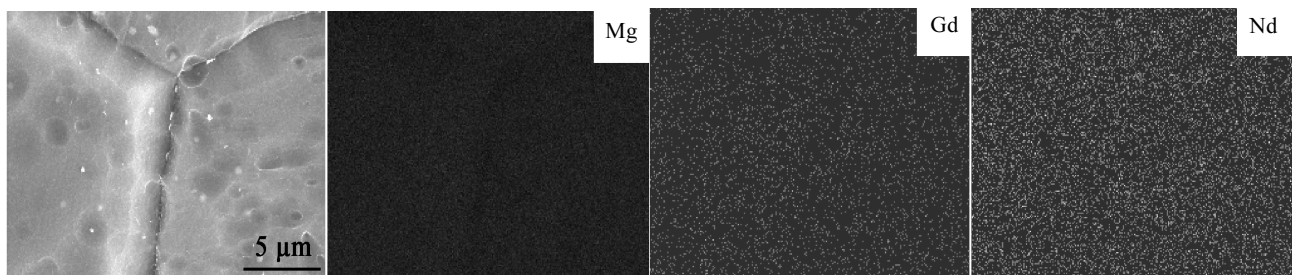


Fig.5 SEM image of extruded alloy and corresponding EDX maps showing the distribution of alloying elements Mg, Gd, and Nd

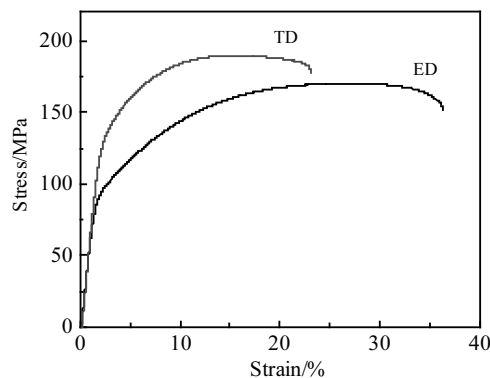


Fig. 6 Tensile stress-strain (*S-S*) curves of the extruded alloy sheet tested along extrusion direction (ED) and transverse direction (TD)

along the TD, while the TD reveals absolutely high strength. The (*S-S*) curve of ED exhibits a gradual strain hardening behavior subsequently to yielding, followed by muted strain softening prior to failure. Yet for the TD the (*S-S*) curve displays an enhanced strain hardening rate and a minor strain softening after the peak stress. Additionally, the extruded alloy reveals excellent plasticity with elongations of 35.2% along ED and 20.5% along TD. It is consistent with the texture observation (as presented in Figs. 3 and 4), where the weaker the texture is, the better the plasticity would be. This occurred because the broader spread in orientations results in effective activation of basal and non-basal slip systems which facilitates plastic deformation and allows the alloy to accommodate larger strains prior to failure^[33]. The continuous strain hardening behavior along the ED is in good agreement with this. On the other hand, the texture is responsible for the planar anisotropy of the extruded alloy. Basal slip is the principle deformation mechanism in magnesium alloys. With consideration to the inverse pole figures (Fig. 4) of the extruded alloy, the orientation distribution of grains in the ED reveals an additional shift from the arc between the $\langle 10\bar{1}0 \rangle$ and $\langle 11\bar{2}0 \rangle$ poles. That is, it produces an additional angle between the optimal slip direction and the tensile direction, resulting in lower deformation resistance of the grains. The reduced flow stress and strain hardening rate along the ED is definitely confirmed.

3 Conclusions

1) The as-cast Mg-1Gd-1Nd alloy exhibits a eutectic microstructure with α -Mg solid solution and semi-continuous eutectic phase. Subsequently to solution treatment, the coarse eutectic phase is mostly dissolved in the matrix.

2) Hot extrusion put significant effect on the grain

refinement of the Mg-1Gd-1Nd alloy. Additionally, a weak texture characterized by the basal pole spread, towards both the ED and TD of the extruded sheet, is obtained. The orientation distribution of grains in the ED is more dispersive than in the TD.

3) The highly refined microstructure and weak texture lead to enhanced plasticity of the extruded alloy. On the other hand, the texture results in planar anisotropy of the alloy sheet that the ED possesses higher elongation while the TD reveals higher strength.

References

- 1 Pollock T M. *Science*[J], 2010, 328: 986
- 2 Yu Kun, Xiong Hanqing, Dai Yilong et al. *Rare Metal Materials and Engineering*[J], 2017, 46(3): 622
- 3 Chen Xianhua, Geng Yuxiao, Pan Fusheng. *Rare Metal Materials and Engineering*[J], 2016, 45(1): 13
- 4 Fores F H, Eliezer D, Aghion E. *Journal of the Minerals Metals and Materials Society*[J], 1998, 50(9): 30
- 5 Mordike B L, Ebert T. *Materials Science and Engineering A*[J], 2001, 302: 37
- 6 Zeng Z R, Zhu Y M, Xu S W et al. *Acta Materialia*[J], 2016, 105: 479
- 7 Lentz M, Nissen J, Fahrenson C et al. *Materials Science and Engineering A*[J], 2016, 655: 17
- 8 Jung I H, Sanjari M, Kim J, Yue S. *Scripta Materialia*[J], 2015, 102: 1
- 9 Stanford N, Barnett M R. *Scripta Materialia*[J], 2008, 58(3): 179
- 10 Stanford N, Barnett M R. *Materials Science and Engineering A*[J], 2008, 496(1-2): 399
- 11 Stanford N. *Materials Science and Engineering A*[J], 2010, 527: 2669
- 12 Al-Samman T, Li X. *Materials Science and Engineering A*[J], 2011, 528(10-11): 3809
- 13 Yan H, Chen R S, Han E H. *Materials Science and Engineering A*[J], 2010, 527: 3317
- 14 Tekumalla S, Yang C, Seetharaman S et al. *Journal of Alloys and Compounds*[J], 2016, 689: 350
- 15 Ball E A, Prangnell P B. *Scripta Metallurgica Materialia*[J], 1994, 31(2): 111
- 16 Mackenzie L W F, Davis B, Humphreys F J et al. *Materials Science and Technology*[J], 2007, 23(10): 1173
- 17 Basu I, Al-Samman T, Gottstein G. *Materials Science and Engineering A*[J], 2013, 579: 50
- 18 Basu I, Al-Samman T. *Acta Materialia*[J], 2014, 67: 116
- 19 Hantzsche K, Bohlen J, Wendt J et al. *Scripta Materialia*[J], 2010, 63: 725
- 20 Xiao Long, Zhong Yan, Chen Cuiping et al. *Transactions of Nonferrous Metal Society of China*[J], 2014, 24(3): 777
- 21 Ma Q, Li B, Whittington W R et al. *Acta Materialia*[J], 2014, 67: 102
- 22 Sarker D, Chen D L. *Materials Science and Engineering A*[J],

- 2013, 582: 63
- 23 Yi S, Brokmeier H G, Letzig D. *Journal of Alloys and Compounds*[J], 2010, 506(1): 364
- 24 Ma Q, Li B, Marin E B, Horstemeyer S J. *Scripta Materialia*[J], 2011, 65: 823
- 25 Molodov D A, Bozzolo N. *Acta Materialia*[J], 2010, 58: 3568
- 26 Bozzolo N, Dewobroto N, Grosdidier T et al. *Materials Science and Engineering A*[J], 2005, 397: 346
- 27 Hirsch J, Al-Samman T. *Acta Materialia*[J], 2013, 61: 818
- 28 Bohlen Jan, Yi Sangbong, Letzig Dietmar et al. *Materials Science and Engineering A*[J], 2010, 527(26): 7092
- 29 Suh B C, Shim M S, Shin K S et al. *Scripta Materialia*[J], 2014, 84-85: 1
- 30 Sanjari M, Farzadfar A, Kabir A S H et al. *Journal of Materials Science*[J], 2014, 49(3): 1408
- 31 Stanford N, Callaghan M D, de Jong B. *Materials Science and Engineering A*[J], 2013, 565: 459
- 32 Stanford N, Sha G, Xia J H et al. *Scripta Materialia*[J], 2011, 65: 919
- 33 Stanford N, Atwell D, Beer A et al. *Scripta Materialia*[J], 2008, 59(7): 772

Mg-RE 挤压合金晶体学结构与力学性能各向异性分析

翟艺璇, 侯秀丽, 袁志钟, 张 鹏, 关庆丰

(江苏大学, 江苏 镇江 212013)

摘 要: 研究了热挤压加工对 Mg-1Gd-1Nd (质量分数, %) 合金显微组织、织构及力学性能的影响。结果表明, 铸态合金呈现典型的共晶显微组织, 包含 α -Mg 基体及半连续状的共晶化合物。经固溶热处理后, 这些共晶化合物已基本固溶入 α -Mg 基体中。采用电子背散射衍射 (EBSD) 技术分析了挤压合金的显微组织与织构。结果表明, 挤压合金显示出了完全再结晶的显微组织与弱的基面织构。合金中的晶粒基面同时朝向挤压板材的挤压方向与垂直方向偏移, 尤其在挤压方向上晶粒的取向更加分散。这种分散的取向可以有效地激活合金中的基面滑移使得合金在断裂前能够承受更大的塑性变形。另一方面, 织构也影响了合金力学性能的各向异性。

关键词: 镁合金; 稀土; EBSD; 织构; 力学性能

作者简介: 翟艺璇, 女, 1993 年生, 硕士生, 江苏大学材料科学与工程学院, 江苏 镇江 212013, 电话: 0511-88797887, E-mail: houxili@ujs.edu.cn